DOI: 10.1021/ma9012829

Macromolecules
ARTICLE

Nitroxide-Mediated Radical Polymerization of Styrene in Aqueous Microemulsion: Initiator Efficiency, Compartmentalization, and Nitroxide Phase Transfer

Per B. Zetterlund,*,†,‡ Junpei Wakamatsu,† and Masayoshi Okubo*,†

†*Department of Chemical Science and Engineering, Graduate School of Engineering, Kobe University, Kobe 657-8501, Japan.* ‡*Current address: Centre for Advanced Macromolecular Design (CAMD), School of Chemical Sciences and Engineering, The University of New South Wales, Sydney, NSW 2052, Australia*

Received June 15, 2009; Revised Manuscript Received July 20, 2009

ABSTRACT: Nitroxide-mediated radical polymerizations (NMP) of styrene at 100 °C using the cationic emulsifier tetradecyltrimethylammonium bromide (TTAB) have been carried out employing 2,2′-azoisobutyronitrile (AIBN) and two nitroxides of different water solubilities. The polymerization rate was lower and the molecular weight distribution more narrow in microemulsion than bulk at low conversion. The results can be rationalized based on the lower initiator efficiency in microemulsion than bulk, presumably caused by the confined space effect (compartmentalization) on geminate termination of AIBN radicals, and possibly also the confined space effect causing an increase in deactivation rate. The extent of retardation relative to bulk was more severe for the less water-soluble 2,2,5-trimethyl-4-phenyl-3-azahexane-3-oxy (TIPNO) than the more water-soluble *N*-*tert*-butyl-*N*-[1-diethylphosphono-(2,2-dimethylpropyl)] nitroxide (SG1) as expected based on more extensive nitroxide exit occurring in the case of SG1 than TIPNO. The results illustrate how effects of heterogeneity can profoundly influence the course of NMP in dispersed systems.

Introduction

The field of polymer chemistry has been revolutionized in the past 15 years with the advent of controlled/living radical polymerization (CLRP), which enables precise synthesis of polymer of various architectures.[1] CLRP has now been adapted to be applicable also in a wide range of dispersed systems (e.g., emulsion, miniemulsion, microemulsion),[2,3] although a number of challenges still remain.

One such challenge is to further increase the understanding of, and ultimately exploit, the concept of compartmentalization in CLRP in dispersed systems.[4−15] Compartmentalization refers to the physical isolation of reactants in discrete confined spaces (polymer particles and/or monomer droplets), and comprises two separate effects: The segregation effect and the confined space effect.[6] The segregation effect refers to two species located in separate particles being unable to react, whereas the confined space effect refers to two species reacting more rapidly in a small particle than in a large particle. Theory dictates that for CLRP systems based on the persistent radical effect[16] (e.g., nitroxide-mediated polymerization (NMP[17,18]) and atom transfer radical polymerization (ATRP[19,20])), it is possible to obtain an increase in both the livingness (end-functionality) and control over the molecular weight distribution (MWD) as a result of compartmentalization.[6−8,14,15] Under ideal conditions, the livingness increases as a result of segregation of propagating radicals reducing the termination rate, whereas the confined space effect leads to an increase in the deactivation rate, which in turn results in an increase in the number of activation−deactivation cycles and thus a narrower MWD. Under such circumstances, the polymerization rate (R_p) is reduced relative to the corresponding bulk system.

*Corresponding authors. (P.B.Z.) E-mail: p.zetterlund@unsw.edu.au. Telephone: +61-2-9385 4331; Fax:+61-2-9385 6250. (M.O.) E-mail: okubo@kobe-u.ac.jp. Telephone and fax: +81-78-803-6161.

Experimental data consistent with compartmentalization effects in miniemulsion NMP have been obtained by Cunningham and co-workers for 2,2,6,6-tetramethylpiperidine-*N*-oxyl-(TEMPO-) mediated miniemulsion polymerization of styrene (S) at 135 °C.[9] A decrease in the particle size resulted in a decrease in R_p and an increase in livingness, but the control remained relatively unaffected. No convincing evidence of compartmentalization effects in *N*-*tert*-butyl-*N*-[1-diethylphosphono-(2,2-dimethylpropyl)] nitroxide (SG1) mediated polymerizations in emulsion[13,21] and miniemulsion[22] has to date been reported, most likely because the relatively high water solubility of SG1 counteracts the confined space effect on deactivation[13] and/or the particles have not been sufficiently small. The NMP equilibrium constant is higher for SG1 than TEMPO,[23] resulting in a higher nitroxide concentration for SG1, and thus smaller particles are required for compartmentalization effects to be manifested for SG1.

In general, the heterogeneous polymerization type that yields the smallest particle size is microemulsion polymerization.[24,25] A microemulsion is a thermodynamically stable, macroscopically homogeneous mixture of two immiscible liquids and a surfactant, which forms spontaneously without external shear forces. A microemulsion initially consists of monomer-swollen micelles (diameter (d) = 5−10 nm), and some of these micelles are subsequently converted to polymer particles during the polymerization. Only a fraction of monomer-swollen micelles become nucleated, and the remaining monomer-swollen micelles supply monomer to the growing particles. This process, as well as some degree of coalescence, normally results in polymer particles with d = 20−60 nm.

We have previously reported on microemulsion NMP of S at 125 °C with the cationic surfactant tetradecyltrimethylammonium bromide (TTAB).[26] Use of TEMPO yielded very low R_p, consistent with the confined space effect increasing the rate of deactivation and the rate of geminate termination of spontaneously (thermally) generated radicals from S. However, the

 Published on Web 07/31/2009

Scheme 1. Chemical Structures of SG1 and TIPNO

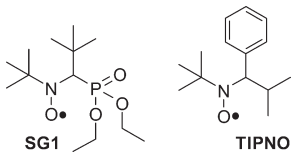

MWDs were broad and the particles were fairly large for a microemulsion (d = 39−129 nm). The broad MWDs are likely to have originated in alkoxyamine decomposition[27] and differing diffusion rates of monomer and low MW alkoxyamines (and nitroxide) between monomer-swollen micelles and polymer particles, causing the ratio [monomer]/[alkoxyamine] to vary between particles. Polymerizations using SG1 proceeded much faster, resulting in d = 21−37 nm and markedly lower M_w/M_n than for TEMPO.

In the present contribution, we have investigated the microemulsion polymerization of S at 100 °C using two nitroxides of different water solubility: SG1 and the much less water-soluble 2,2,5-trimethyl-4-phenyl-3-azahexane-3-oxy (TIPNO; Scheme 1). The experimental work is complemented by modeling and simulations of the effects of compartmentalization using modified two-dimensional Smith−Ewart equations.[6]

Experimental Section

Materials. S was purified by distillation under reduced pressure in a nitrogen atmosphere. 2,2′-Azoisobutyronitrile (AIBN; Wako) was purified by recrystallization. *N*-*tert*-Bbutyl-*N*-[1-diethylphosphono-(2,2-dimethylpropyl)] nitroxide (SG1) was obtained from ARKEMA K.K. (Japan) and was used as received. 2,2,5-Trimethyl-4-phenyl-3-azahexane-3-oxy (TIPNO) was synthesized according to the literature, and purified by column chromatography before use.[28,29] *n*-Tetradecyltrimethylammonium bromide (TTAB; Tokyo Kasei Kogyo Co. Ltd., Tokyo, Japan) and toluene, methanol, and hexadecane (Nacalai Tesque Inc., Kyoto, Japan) were used as received. Deionized water with a specific resistance of 5×10^6 Ω cm was distilled prior to use.

Microemulsion Polymerization. A solution of AIBN (22 mg, 1.35×10^{-4} mol) and SG1 (72 mg, 2.45×10^{-4} mol) in S (10 g, 9.62×10^{-2} mol) was added to an aqueous solution of TTAB (25 g TTAB in 165 g water), followed by magnetic stirring for 15 min at room temperature, resulting in the formation of a transparent solution (microemulsion). The microemulsion was charged in a glass ampule, which was subsequently degassed using several N_2/vacuum cycles and sealed off. Polymerization was conducted at 100 °C under a nitrogen atmosphere. The polymerizations were stopped by gradually reducing the temperature to room temperature using cold water, and the polymer was isolated by addition of excess methanol (leading to coagulation), followed by filtration, and drying. The TIPNO-mediated microemulsion polymerizations were carried out in the same way.

Microemulsion Polymerizations Used To Investigate Partitioning. Two microemulsions were prepared: (A) S (10 g)/AIBN (22 mg)/water (165 g)/TTAB (25 g); (B) S (10 g)/AIBN (22 mg)/TEMPO (50.2 mg)/water (165 g)/TTAB (25 g). Microemulsion A contains no TEMPO, and microemulsion B contains twice the amount of the required TEMPO. On mixing of A and B, the total $[TEMPO]_0/[AIBN]_0$ is 1.2. Microemulsions A and B were subsequently mixed at room temperature and polymerized at 125 °C. The time taken from the moment when A and B were mixed together to the start of the polymerization was approximately 15 min. The polymer was isolated as described above.

Bulk Polymerization. S (20 g; 1.92×10^{-1} mol), AIBN (44 mg; 2.70×10^{-4} mol), and SG1 (143 mg; 4.86×10^{-4} mol) were charged in a glass ampule, which was degassed with several N_2/vacuum cycles, sealed off under vacuum, and heated at 100 °C in an oil bath. The polymer was recovered by precipitation in excess methanol, and subsequently purified by reprecipitation using toluene/methanol and dried in a high vacuum oven. The TIPNO-mediated polymerizations were carried out in the same way.

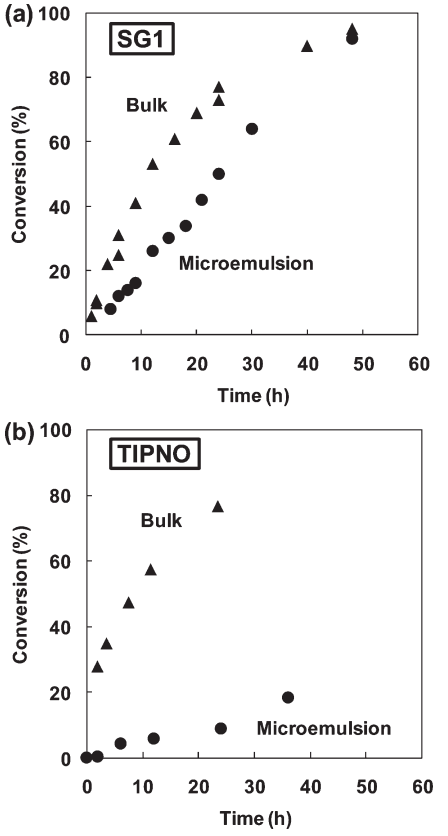

Figure 1. Conversion vs time for nitroxide-mediated polymerization of styrene at 100 °C with $[nitroxide]_0/[AIBN]_0$ = 1.8 for nitroxides (a) SG1 and (b) TIPNO in bulk and microemulsion.

Measurements. S conversions were determined by gas chromatography (Shimadzu Corporation, GC-18A) with helium as carrier gas, employing *N*,*N*-dimethylformamide as solvent and *p*-xylene as internal standard. MWDs were obtained by gel permeation chromatography (GPC) employing a Tosoh GPC system equipped with two TSK gel columns (GMHHR-H, 7.8 mm i.d. 30 cm) using tetrahydrofuran (THF) as eluent at 40 °C at a flow rate of 1.0 mL min^{-1}, and a refractive index detector (RI-8020). The column was calibrated against five standard PS samples (1.05×10^3 to 5.48×10^6 g/mol). Particle size distributions were measured using dynamic light scattering (DLS; FPAR-1000, Otsuka Electronics, Osaka, Japan) at a light scattering angle of 160° at 25 °C. Number-average (d_n) and weight-average (d_w) droplet diameters were obtained using the Marquadt analysis routine (d_w/d_n = 1.1−1.3).

Results and Discussion

SG1-Mediated Polymerizations in Microemulsion and Bulk. SG1-mediated microemulsion polymerization of S using the cationic surfactant TTAB were carried out as well as the corresponding bulk polymerization (the same organic phase as in microemulsion) with $[SG1]_0/[AIBN]_0$ = 1.80 at 100 °C. The microemulsion polymerization proceeded at a significantly lower rate than the bulk polymerization (Figure 1a). The initial microemulsion was transparent, but the emulsion became translucent and whitish with increasing conversion (Figure 2). DLS measurements revealed that the

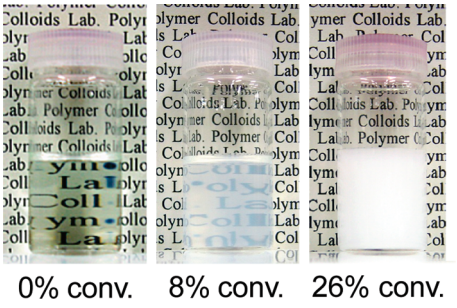

Figure 2. Microemulsions at various conversions for SG1-mediated polymerization of styrene at 100 °C with $[SG1]_0/[AIBN]_0 = 1.8$.

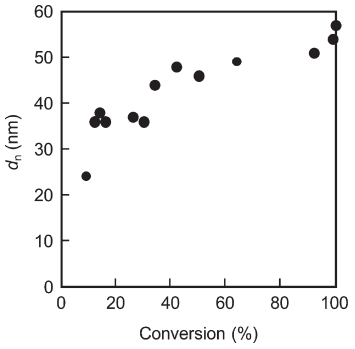

Figure 3. Number-average particle diameters (d_n) for SG1-mediated polymerization of styrene at 100 °C with $[SG1]_0/[AIBN]_0 = 1.8$.

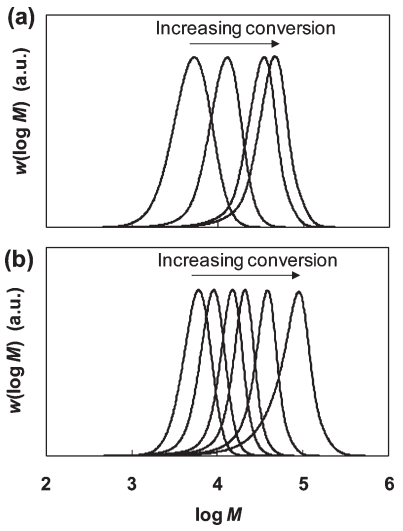

Figure 4. Molecular weight distributions (normalized to peak height) for SG1-mediated polymerization of styrene at 100 °C with $[SG1]_0/[AIBN]_0 = 1.8$ in (a) bulk (conversion 10, 25, 77, 95%) and (b) microemulsion (conversion 8, 12, 16, 26, 42, 92%).

particle size gradually increased with increasing conversion from $d_n \approx 23$ to 55 nm (Figure 3).

Both in microemulsion and bulk, the MWDs shifted to higher molecular weight (MW) with increasing conversion, indicating good livingness (Figure 4). The values of M_n increased close to linearly with conversion in both microemulsion and bulk (Figure 5a). However, M_n was significantly greater in microemulsion than in bulk. The values of M_w/M_n in bulk initially decreased, went through a minimum value, and finally increased at high conversion (Figure 5b), which is normal behavior. In the microemulsion, M_w/M_n increased closed to linearly with conversion in a manner

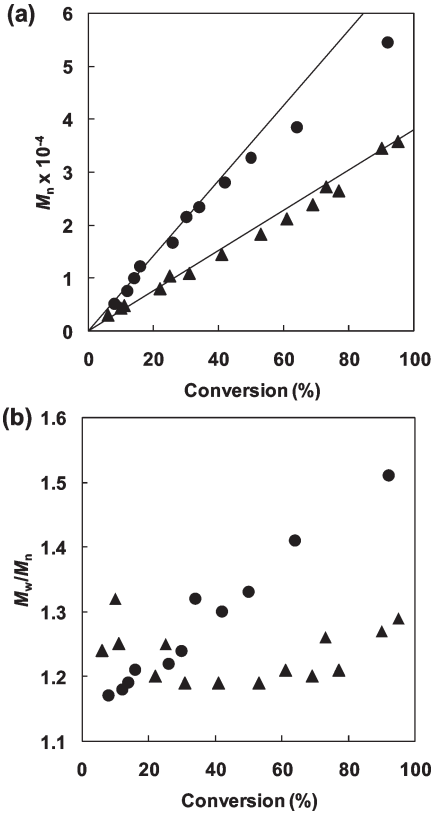

Figure 5. Number average molecular weights (M_n) (a) and polydispersities (M_w/M_n) (b) vs conversion for SG1-mediated polymerization of styrene at 100 °C with $[SG1]_0/[AIBN]_0 = 1.8$ in bulk (triangles) and microemulsion (circles). The lines in part a are theoretical M_n based on initiator efficiencies (f) of AIBN of 0.98 for bulk and 0.53 for microemulsion.

distinctly different from in bulk. For conversions below approximately 20%, M_w/M_n was lower in microemulsion than in bulk, whereas the control in bulk was superior at higher conversions. Figure 6 shows an overlay of MWDs for bulk and microemulsion at similar MWs, revealing a much narrower MWD in microemulsion. For example, for $M_n \approx 5000$ g mol^{-1}, $M_w/M_n = 1.17$ in microemulsion to be compared with 1.32 in bulk.

Three factors will now be considered to rationalize the data: Initiator efficiency, monomer concentration at polymerization locus, and compartmentalization.

Initiator Efficiency. In the case of an excess nitroxide as in the present work, the theoretical M_n ($M_{n,th}$) is calculated from the ratio of consumed monomer units to radicals generated from decomposition of AIBN (i.e., not relative to nitroxide): $M_{n,th} = ([S]_0 \alpha M_S)/[R^\bullet]_{gen}$, where α is S conversion, M_S is the molar mass of S, and $[R^\bullet]_{gen}$ is the total concentration of radicals generated by AIBN decomposition ($= 2f\,[AIBN]_0$, where f is the initiator efficiency). The linear relationships between M_n and α in Figure 5a were fitted at low conversion based on the above equations to give $f = 0.53$ for microemulsion and $f = 0.98$ for bulk. The value in bulk is higher than expected for reasons that are not clear. However, the important message is that f in microemulsion is much less than in bulk. The reason $f < 1$ is that some fraction of the cyanoisopropyl radicals engage in side reactions other than addition to monomer, e.g. geminate termination. The present data thus indicate that such side reactions are more prevalent in microemulsion than bulk. An additional factor may be exit of AIBN radicals followed by aqueous phase termination.

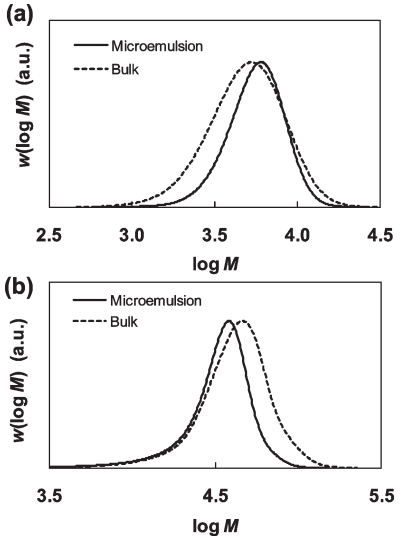

Figure 6. Molecular weight distributions (normalized to peak height) for SG1-mediated polymerization of styrene at 100 °C with $[SG1]_0/[AIBN]_0 = 1.8$ in microemulsion (full lines) and bulk (dotted lines). (a) Microemulsion: $M_n = 5100$ g mol^{-1}, $M_w/M_n = 1.17$, 8% conversion (4.5 h). Bulk: $M_n = 4200$ g mol^{-1}, $M_w/M_n = 1.32$, 10% conversion (2 h). (b) Microemulsion: $M_n = 27900$ g mol^{-1}, $M_w/M_n = 1.1.30$, 42% conversion (21 h). Bulk: $M_n = 35700$ g mol^{-1}, $M_w/M_n = 1.29$, 95% conversion (48 h).

The rate of geminate termination would be expected to be higher in a sufficiently small particle than in bulk as a result of the confined space effect, which would explain f(microemulsion) < f(bulk).[4,6,30−32] This explanation is consistent with M_n vs conversion being close to linear in both cases, because the events that dictate the slope occur at very low conversion when the AIBN decomposes (at 100 °C, 95% decomposes in less than 3 min). Interestingly, f(microemulsion) < f(bulk) also indicates that enhanced spontaneous initiation in microemulsion relative to bulk does not appear to be a factor with regards to f (enhanced spontaneous initiation would result in an apparent increase in f, possibly above unity). It has previously been shown that the rate of spontaneous initiation of S in aqueous miniemulsion at 110 and 125 °C is markedly greater than in bulk.[33] However, it may be that there is enhanced initiation relative to bulk, but that these radicals, if generated in pairs, undergo rapid geminate termination due to the confined space effect. Alternatively, the rate of (enhanced) spontaneous initiation may be relatively low at 100 °C.

The lower value of f in microemulsion means that there is a greater excess of free nitroxide in microemulsion than in bulk, which would result in lower R_p and better control/livingness. In order to quantify this effect, simulations were carried out for a homogeneous system (bulk), varying the value of f, using the software PREDICI[34] based on eqs 1−7:

$$\frac{d[I]}{dt} = -k_d[I] \quad (1)$$

$$\frac{d[M]}{dt} = -k_p[P^\bullet][M] - k_i[R^\bullet][M] - 3k_{i,th}[M]^3 \quad (2)$$

$$\frac{d[PT]}{dt} = k_{deact}[P^\bullet][T^\bullet] - k_{act}[PT] \quad (3)$$

$$\frac{d[RT]}{dt} = k_{deact}[R^\bullet][T^\bullet] - k_{act}[RT] \quad (4)$$

Table 1. Literature Rate Coefficients for Activation (k_{act}) and Deactivation (k_{deact}) of 1-Phenylethyl−SG1 and 1-Phenylethyl−TIPNO at 120 °C

nitroxide	k_{act} (s^{-1})[37]	k_{deact} (M^{-1} s^{-1})[48]	K ($=k_{act}/k_{deact}$)
SG1	5.5×10^{-3}	4.6×10^{6}	1.2×10^{-9}
TIPNO	3.3×10^{-3}	8.2×10^{6}	4.0×10^{-10}

$$\frac{d[P^\bullet]}{dt} = k_{act}[PT] - k_{deact}[P^\bullet][T^\bullet] - 2k_t[P^\bullet]^2 - k_t[R^\bullet][P^\bullet] \quad (5)$$

$$\frac{d[T^\bullet]}{dt} = k_{act}[PT] - k_{deact}[P^\bullet][T^\bullet] - k_{deact}[R^\bullet][T^\bullet] \quad (6)$$

$$\frac{d[R^\bullet]}{dt} = 2fk_d[I] + k_{act}[RT] + k_{i,th}[M]^3 - k_i[R^\bullet][M] - 2k_t[R^\bullet]^2 - k_t[R^\bullet][P^\bullet] - k_{deact}[R^\bullet][T^\bullet] \quad (7)$$

where $R^\bullet$ denotes "small radicals" (cyanoisopropyl radicals from AIBN decomposition and radicals generated by thermal initiation of S[35,36]), $T^\bullet$ is nitroxide, $P^\bullet$ denotes propagating radicals, PT denotes oligomeric/polymeric alkoxyamine, RT is low MW alkoxyamine, M is monomer, and I is initiator. This model represents an ideal NMP mechanism for a system that starts with free nitroxide and a radical initiator, not accounting for side reactions such as e.g. nitroxide[37,38] and alkoxyamine[27] decomposition. Parameter values (100 °C): k_d(AIBN) = 1.41×10^{-3} s^{-1};[39] $k_p = 1200$ M^{-1} s^{-1};[40] $k_t = 1.46 \times 10^{8}$ M^{-1} s^{-1};[41] $k_{i,th} = 1.62 \times 10^{-11}$ M^{-2} s^{-1};[35] $k_i = 1.08 \times 10^{4}$ M^{-1} s^{-1}.[42] The reported Arrhenius parameters (A_{act} and E_{act}) of k_{act} of S/SG1[43] (polymeric alkoxyamine, unlike Table 1) give $k_{act} = 1.25 \times 10^{-3}$ s^{-1} at 100 °C. The value of k_{deact} was taken as 6.8×10^{5} M^{-1} s^{-1}, which has been reported for the polymeric system at 80 °C[44] (radical coupling reactions have weak temperature dependence), resulting in K ($=k_{act}/k_{deact}$) = 1.84×10^{-9} M. All rate coefficients involving $P^\bullet$ and $R^\bullet$ were assumed to be the same (except for k_i and k_p). Simulations were carried out with $f = 0.98$ and 0.53, with $[M]_0 = 8.7$ M, $[I]_0 = 1.21 \times 10^{-2}$ M, and $[T^\bullet]_0 = 2.20 \times 10^{-2}$ M. All rate coefficients were assumed to be independent of chain-length and conversion. This introduces an error due to k_t conversion dependence.[45−47] However, the purpose of the simulations is to quantify the effect of f, the relative extent of which will not be significantly affected by k_t conversion dependence. Termination was assumed to occur by combination only.

Simulated conversion−time and MWDs are shown in Figure 7 for $f = 0.98$ and 0.53, confirming that R_p is lower and the MWD is narrower for $f = 0.53$ than 0.98, as expected. The results are in semiquantitative agreement with experimental data (Figures 1a and 6). Thus, one important contributing factor to lower R_p and narrower MWD in microemulsion than bulk is the lower value of f in microemulsion, presumably caused mainly by the confined space effect on geminate termination of AIBN radicals.

Monomer Concentration at Polymerization Locus. When comparing microemulsion and bulk NMP, an additional possible factor is that in the microemulsion system, some fraction of monomer resides in monomer-swollen micelles that have not been nucleated, and these micelles act as monomer reservoirs similar to in an emulsion polymerization. The average monomer concentration at the locus of polymerization at a given conversion is therefore lower than in the corresponding bulk system, which would result in a reduction in R_p in microemulsion. In theory, this would also

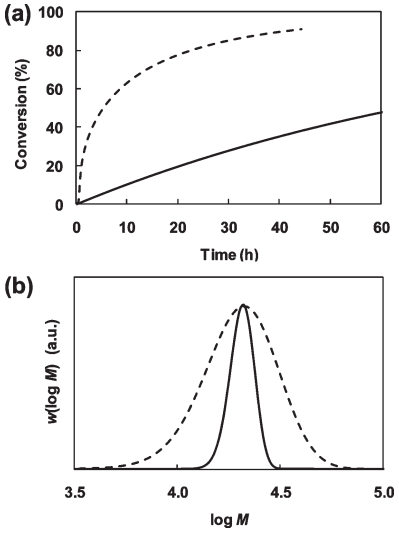

Figure 7. Simulated conversion−time (a) and MWDs (b) for nitroxide-mediated polymerization of styrene at 100 °C with $[SG1]_0/[AIBN]_0$ = 1.8 in bulk with f = 0.98 (dotted lines) and 0.53 (full lines).

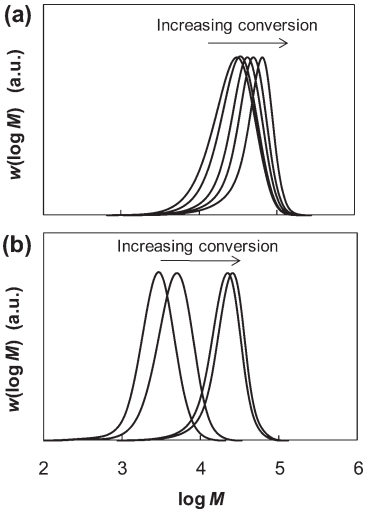

Figure 8. Molecular weight distributions (normalized to peak height) for TIPNO-mediated polymerization of styrene at 100 °C with $[TIPNO]_0/[AIBN]_0$ = 1.8 in (a) bulk (conversion 28, 35, 47, 58, 76%) and (b) microemulsion (conversion 4, 6, 9, 18%).

lead to a narrowing of the MWD as fewer monomer units would be added per activation−deactivation cycle. However, this effect is believed to be relatively minor.

Compartmentalization. We next consider effects of compartmentalization. In a conventional, nonliving microemulsion polymerization, R_p is much greater than in bulk.[24,25] In such a system, there is no deactivation reaction as in CLRP, and segregation of propagating radicals leads to an increase in R_p. Segregation is expected to operate also in microemulsion NMP.[6,8,14] However, if the confined space effect exerts a stronger influence on R_p than segregation, the net effect will be a decrease in R_p.[6,14] Compartmentalization effects are discussed in more detail later in this article.

Theory on compartmentalization in NMP in dispersed systems dictates that a decrease in R_p is accompanied by a reduction in M_w/M_n.[6,8,14] The microemulsion system did exhibit lower M_w/M_n than in bulk at low conversion, but at higher conversions, M_w/M_n(microemulsion) > M_w/M_n bulk). Mainly three reasons can be conceived of to rationalize the MWDs being broader in microemulsion than bulk at higher conversions:[26] (*i*) Diffusion of monomer from nonnucleated monomer-swollen micelles to polymer particles would give rise to different ratios [monomer]/[alkoxyamine] in different particles, and thus different M_n in different particles. (*ii*) On the basis of an initial monomer-swollen micelle radius of 8 nm, one micelle would contain approximately three alkoxyamine species after AIBN decomposition. With such a low average number, there would be considerable variation in the number of alkoxyamines between different particles, resulting in different M_n in different particles. (*iii*) Due to the relatively low R_p in microemulsion, alkoxyamine decomposition[27] would play a more significant role than in the bulk.

TIPNO-Mediated Polymerizations. TEMPO-mediated microemulsion polymerization of S at 125 °C is severely retarded relative to bulk,[26] in contrast with the present SG1 results where only fairly mild retardation was observed (Figure 1a). From the viewpoint of compartmentalization, this would suggest that the confined space effect is weaker for SG1 than TEMPO. SG1 is considerably more water-soluble than TEMPO, and it is possible that exit of SG1 counteracts the confined space effect on deactivation. To test this hypothesis, microemulsion NMP was carried out using the nitroxide TIPNO (Scheme 1), which has similar activation (k_{act}) and deactivation (k_{deact}) rate coefficients to SG1 (Table 1), but is expected to be considerably less water-soluble. One would thus anticipate a stronger confined space effect, and thus lower R_p, for TIPNO than SG1.

Figure 1b shows conversion−time data for the TIPNO-mediated microemulsion and bulk polymerizations of S at 110 °C with $[TINPO]_0/[AIBN]_0$ = 1.80. The polymerizing microemulsion was transparent/translucent with $d_n \approx 20-25$ nm. The microemulsion polymerization was very strongly retarded, much more so than in the case of SG1 (Figure 1a). The MWDs were narrow and shifted to higher MW with increasing conversion both in microemulsion and bulk (Figure 8). Similarly to in the case of SG1, at $M_n \approx 20{,}000$ g mol^{-1}, the MWD was considerably narrower in microemulsion than in bulk (M_w/M_n = 1.30 compared to 1.56; Figure 9), as also indicated by the M_w/M_n values in Figure 10. The M_n data also indicate that f(microemulsion) < f(bulk) also for TIPNO, although the scatter in the data precludes meaningful estimation of f in microemulsion.

These observations are consistent with expectation based on TIPNO being less water-soluble than SG1, thus resulting in a stronger confined space effect on deactivation and therefore lower R_p than for SG1.

Nitroxide Phase Transfer. In order to investigate the ability of nitroxide to undergo phase transfer, two S microemulsions, A and B, were prepared. A and B were identical, except that A contained no TEMPO and B contained twice the amount of TEMPO based on $[TEMPO]_0/[AIBN]_0$ = 1.2. Mixing of A and B thus results in a microemulsion with $[TEMPO]_0/[AIBN]_0$ = 1.2. The results of this "mixing" preparation was then compared with a microemulsion prepared in the normal way with $[TEMPO]_0/[AIBN]_0$ = 1.2.

Figure 11 shows conversion−time, M_n and M_w/M_n data of both polymerizations at 125 °C, revealing virtually identical results (within experimental error). These results clearly show that TEMPO is able to exit from one particle (monomer−swollen micelle), diffuse through the aqueous phase, and enter another particle, and that the time taken for this diffusive process is less than 15 min (i.e., the time taken after initial mixing of A and B until the start of the polymerization). These findings are consistent with theoretical work by Cunningham and co-workers, who found that phase

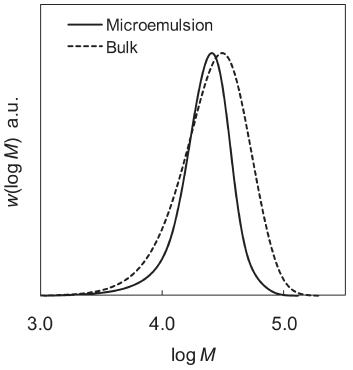

Figure 9. Molecular weight distributions (normalized to peak height) for TIPNO-mediated polymerization of styrene at 100 °C with $[TIPNO]_0/[AIBN]_0 = 1.8$ in microemulsion (full line) and bulk (dotted line). Microemulsion: $M_n = 19300$ g mol^{-1}, $M_w/M_n = 1.30$, 18% conversion (36 h). Bulk: $M_n = 20200$ g mol^{-1}, $M_w/M_n = 1.56$, 28% conversion (2 h).

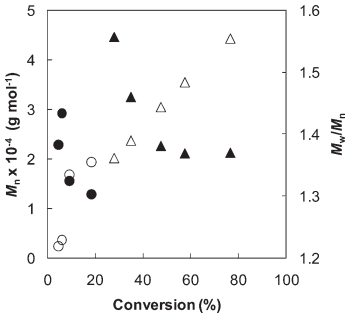

Figure 10. Number average molecular weights (M_n; open symbols) and polydispersities (M_w/M_n; filled symbols) vs conversion for TIPNO-mediated polymerization of styrene at 100 °C with $[TIPNO]_0/[AIBN]_0 = 1.8$ in bulk (triangles) and microemulsion (circles).

equilibrium with respect to TEMPO is reached very rapidly ($< 10^{-4}$ s) under typical miniemulsion NMP conditions, even at high conversion.[49] However, our experiment does not provide information as to whether nitroxide exit can compete with deactivation in any given particle. Charleux showed theoretically that for TEMPO, exit is much faster than deactivation unless $d < 20$ nm.[13] For SG1, which is more water-soluble than TEMPO, exit by far dominates (>98%) even for particles with $d = 10$ nm.[13] Given the above, it is likely that exit is faster than deactivation in the present TEMPO and SG1 microemulsion polymerizations.

With regards to nitroxide water solubility, one must distinguish between two separate effects: (*i*) Nitroxide partitioning. This simply refers to the overall fractions of nitroxide that are located in the organic and aqueous phases. For NMP that proceeds in the nonstationary state under normal conditions (e.g., S/SG1 and S/TIPNO, but not S/TEMPO[23]), this leads to an increase in R_p and decrease in control/livingness.[50] (*ii*) Exit of nitroxide. This refers to the effect on the polymerization in a given particle if exit of nitroxide occurs. The effect of exit depends on the overall nitroxide concentration, i.e. the number of nitroxide species in the particle. If the concentration is so high that each particle contains say 3−4 nitroxide species or more, then exit, followed by entry into another particle, would only have a minor effect on the kinetics. However, if the concentration is so low such that an average particle contains 2 or only 1 nitroxide species, then exit would have a more significant effect. If a particle containing 1 propagating radical and 1 nitroxide experiences exit of nitroxide, the remaining propagating radical would propagate rapidly until chain transfer to monomer occurs or until another nitroxide enters the particle (which may exit before deactivation). This would cause an increase in R_p and a reduction in control/livingness, and counteract the confined space effect.

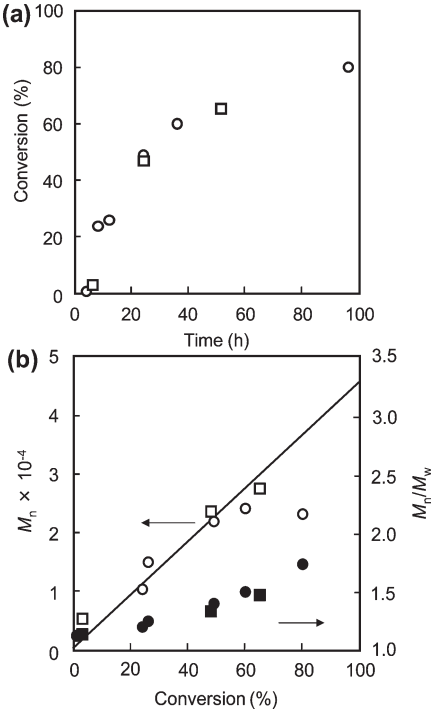

Figure 11. TEMPO-mediated microemulsion polymerization of styrene at 125 °C (5 wt % styrene; $[TEMPO]_0/[AIBN]_0 = 1.2$) using "normal" (circles) microemulsion preparation and "mixing" preparation (squares; see text for details): (a) conversion vs time; (b) M_n (open symbols) and M_w/M_n (filled symbols) vs conversion. The line in is the theoretical M_n ($M_{n,th}$) based on AIBN initiator efficiency (f) = 0.6.

Despite R_p in bulk being almost the same for SG1 and TIPNO, R_p in microemulsion was much lower for TIPNO than SG1 (Figure 1). If nitroxide partitioning, not exit of nitroxide, were the main reason for R_p(microemulsion) being lower for TIPNO than SG1, then one would not expect the MWD to be more narrow in microemulsion than bulk for SG1. It thus seems reasonable to conclude that the main reason for the much stronger retardation in microemulsion for TIPNO than SG1 is related to exit of nitroxide, i.e., the competition between nitroxide exit and deactivation. On the basis of the expected water solubilities, exit would occur more rapidly for SG1 than TIPNO.

In view of the above, it is of interest to estimate the average number of propagating radical and nitroxide species per particle, $\bar{n}_{P^\bullet}$ and $\bar{n}_{T^\bullet}$. A very rough approach (shortcomings detailed below) is to employ eqs 8 − 11:

$$\ln \frac{[M]_0}{[M]} = k_p[P^\bullet]t \tag{8}$$

$$K = \frac{[P^\bullet][T^\bullet]}{[PT]} \tag{9}$$

where t is time, and using $k_p = 1200$ M^{-1} s^{-1}[40] and K(SG1) = 1.84×10^{-9} M (see PREDICI section above). The value of K(TIPNO) was taken to be 1/3 x K(SG1) ($= 6 \times 10^{-10}$ M) based on the values in Table 1 for low MW alkoxyamines. $[M]_0$ and [M] are the initial and instantaneous monomer

concentrations in the organic phase, respectively. Equation 8 gives [P•] (from the initial slope), which is inserted into eq 9 to yield [T•]. The value of [PT] was estimated from the slope of M_n vs conversion (Figure 5a; i.e., via f, which gives the number of initial alkoxyamine species generated), yielding [PT] ≈ 0.013 M for both SG1 and TIPNO. The values of $\bar{n}_{p\bullet}$ and $\bar{n}_{T\bullet}$ are then obtained from eqs 10 and 11:

$$\bar{n}_{T\bullet} = N_A v_p [T^\bullet] \quad (10)$$

$$\bar{n}_{P\bullet} = N_A v_p [P^\bullet] \quad (11)$$

where N_A is Avogadro's number and v_p is the particle volume, taken as corresponding to d = 23 nm, resulting in: SG1: $\bar{n}_{p\bullet} = 1.8 \times 10^{-5}$, $\bar{n}_{T\bullet} = 19$; TIPNO: $\bar{n}_{p\bullet} = 3.6 \times 10^{-6}$, $\bar{n}_{T\bullet} = 1.3$.

These calculations rest on two assumptions: (*i*) All of the monomer is available to undergo propagation at any given time. However, monomer located in non-nucleated micelles would be excluded from propagation and should thus not be included in the first-order plot. For this very same reason, a first-order plot cannot be applied to an emulsion polymerization in intervals I and II. This leads to underestimation of [P•] (because the organic phase $[M]_0/[M]$ as estimated from overall monomer conversion is too low, also including monomer not available to react) and thus overestimation of [T•] and $\bar{n}_{T\bullet}$. (*ii*) The NMP equilibrium constant in a homogeneous system is applicable. If the confined space effect is operative, the deactivation rate is significantly increased, and thus K decreases.[6] It follows that assumption *ii* also leads to overestimation of $\bar{n}_{T\bullet}$. The above estimates of $\bar{n}_{T\bullet}$ can at best be considered very rough estimates of upper limits of $\bar{n}_{T\bullet}$.

It can thus be concluded that $\bar{n}_{T\bullet}$ is likely to be low enough for nitroxide exit to influence the polymerization kinetics. A fundamental criterion for the confined space effect on deactivation to be operative is that some particles contain no nitroxide, i.e. that (approximately) $\bar{n}_{T\bullet} < 1$.[14] This seems very likely to be the case for TIPNO simply based on the upper limit of $\bar{n}_{T\bullet} = 1.3$ (see above). In the case of SG1, the upper limit of $\bar{n}_{T\bullet} = 19$ cannot be invoked to support the existence of a confined space effect on deactivation.

We have previously reported an interface effect in TEMPO-mediated miniemulsion polymerization of S at 125 °C, according to which some fraction of TEMPO is located near/adsorbed at the interface, leading to a reduction in deactivation rate, higher R_p and (partial) loss of control/livingness.[51,52] This effect was observed for particles too large for compartmentalization to be significant. It has also been reported that enhanced spontaneous (thermal) initiation of S related to the oil−water interface,[33] as well as radical generation involving the surfactant sodium dodecylbenzenesulfonate (SDBS),[53] may lead to increased R_p relative to bulk in S/TEMPO miniemulsion. In the present microemulsion polymerizations using nitroxides SG1 and TIPNO, rate enhancement relative to bulk was not observed, indicating that the above effects played only a minor role, if any at all, in comparison with compartmentalization (and other unknown effects).

Modeling of Compartmentalization. Modeling and simulations of nitroxide-mediated polymerization of S in a dispersed system at 100 °C was carried out using our previously developed approach based on two-dimensional Smith−Ewart equations, which account for compartmentalization of both propagating radicals and nitroxide. The approach itself and the underlying assumptions have been reported in detail elsewhere.[6,8,14] The modified Smith−Ewart equations

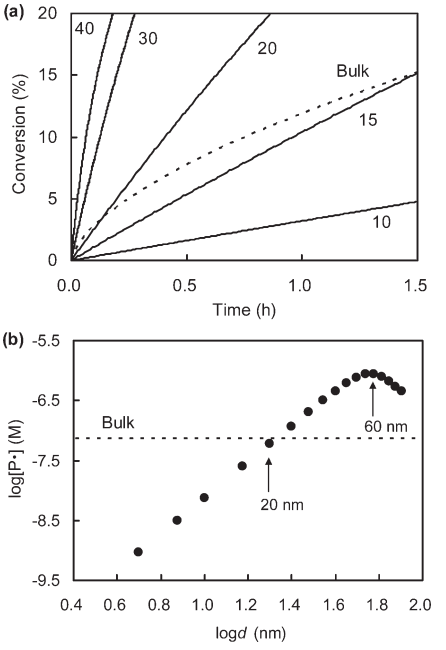

Figure 12. (a) Simulated conversion vs time for different particle diameters (in nm as indicated) for SG1-mediated radical polymerization of styrene in dispersed system at 100 °C (thermal initiation included; $[PT]_0$ = 0.013 M). The thick line denotes simulated bulk conditions. (b) Simulated propagating radical concentrations vs particle diameter at 1% styrene conversion for the conditions in part a. The dotted lines denote the simulated propagating radical concentration under bulk conditions.

describe the number fractions of particles N_i^j (particles containing iP• and jT•):

$$\frac{dN_i^j}{dt} = N_A v_p k_{act}[PT]\{N_{i-1}^j - N_i^j\} + 0.5k_{i,th}[S]^3 N_A v_p \{N_{i-2}^j - N_i^j\} + \frac{k_t}{N_A v_p}\{(i+2)(i+1)N_{i+2}^j - (i)(i-1)N_i^j\} + \frac{k_{deact}}{N_A v_p}\{(i+1)(j+1)N_{i+1}^{j+1} - (i)(j)N_i^j\} \quad (12)$$

where k_t is the termination rate coefficient, and $k_{i,th}$ is the rate coefficient for spontaneous (thermal) initiation of S. The simulations were not taken beyond 20% monomer conversion, thus justifying the use of conversion-independent values of k_p, k_t and k_{deact}.[45−47] The values of k_{act} and k_{deact} for PS-SG1 were employed in the simulations (as above: $k_{act} = 1.25 \times 10^{-3}$ M^{-1}; $k_{deact} = 6.8 \times 10^5$ M^{-1} s^{-1}). On the basis of the rate coefficients for the low MW adducts of SG1 and TIPNO in Table 1, it can be expected that the rate coefficients for TIPNO are very similar. Other rate coefficients: $k_{i,th} = 1.62 \times 10^{-11}$ M^{-2} s^{-1};[35] $k_t = 1.46 \times 10^8$ M^{-1} s^{-1}.[41]

Equation 12 does not account for phase transfer events, e.g., exit and entry of nitroxide. Moreover, the simulated system comprises alkoxyamine and no free nitroxide at time zero. In the real experimental systems of the present work, the polymerizations start with AIBN and nitroxide, with an excess nitroxide. For these reasons, direct comparison between the experimental results and the simulated data is not possible. However, the simulations nonetheless provide an indication as to what may be expected in the experimental systems based on theory.

Figure 12a shows simulated conversion−time data for various particle sizes, revealing how R_p decreases with decreasing particle size. For $d \leq$ approximately 15 nm, R_p

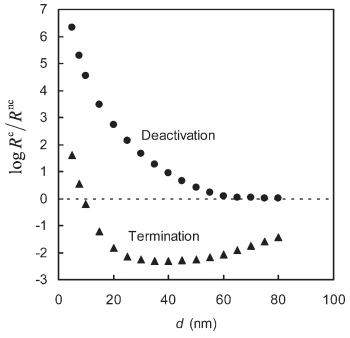

Figure 13. Ratios of "compartmentalized" (R^c) and "non-compartmentalized" (R^{nc}) deactivation (●) and termination (▲) rates for SG1-mediated radical polymerization of styrene in dispersed system at 100 °C (thermal initiation included; $[PT]_0 = 0.013$ M) at 1% styrene conversion.

is lower than in bulk. Figure 12b depicts log[P•] vs log d, showing that there is a particle size range where R_p is significantly greater than in bulk, with the max R_p at $d \approx 60$ nm. When $R_p > R_{p,bulk}$, the segregation effect on termination dominates over the confined space effect on deactivation, leading to lower control (broader MWD) but higher livingness than in bulk. When $R_p < R_{p,bulk}$, both the control and the livingness are superior to bulk.[6,8,14]

Thus, according to theory, very small particles ($d < 20$ nm) are required to obtain a reduction in M_w/M_n relative to bulk. Moreover, it is assumed in the model that the nitroxide does not undergo exit into the aqueous phase. In reality, as addressed above, it is however likely that the nitroxide (in particular SG1) partitions significantly to the aqueous phase,[13] and this would weaken the confined space effect, and thus even smaller particles would be required to obtain an improvement in control over the MWD. In the present experimental work, an improvement in MWD control (lower M_w/M_n) was obtained at low conversion with $d_n < 35$ nm for SG1 (Figure 3) and $d_n \approx 20-25$ nm for TIPNO. Thus, although there is admittedly a slight discrepancy between experiment and theory in terms of absolute particle size, the agreement is at the very least semiquantitative.

The effects of compartmentalization on the individual reactions of deactivation and termination can be assessed using our previously reported approach, whereby in an imaginary experiment, the dispersed phase is instantaneously converted into a continuous bulk phase, and the compartmentalized deactivation and termination rates (R^c) are compared with the corresponding noncompartmentalized rates (R^{nc}) based on eqs 13 - 16:[6,8,14]

$$R_{deact}^{c} = \frac{k_{deact}}{(N_A v_p)^2} \sum_i \sum_j ijN_i^j \quad (13)$$

$$R_t^c = \frac{2k_t}{(N_A v_p)^2} \sum_i \sum_j i(i-1)N_i^j \quad (14)$$

$$R_{deact}^{nc} = k_{deact}[P^\bullet][T^\bullet] \quad (15)$$

$$R_t^{nc} = 2k_t[P^\bullet]^2 \quad (16)$$

Figure 13 shows the termination rate in a compartmentalized system relative to that in the corresponding noncompartmentalized system. Over a wide particle size range, the termination rate is significantly reduced ($R_t^c/R_t^{nc} > 1$ for very small particles is caused by the contribution of geminate termination of radicals from spontaneous initiation of S, which occurs rapidly in small particles due to the confined space effect[6]). At $d = 40$ nm, the termination rate in the compartmentalized system is reduced by a factor of 198 ($R_t^c/R_t^{nc} = 5.05 \times 10^{-3}$) at 1% conversion. Under these conditions, $\bar{n}_{p\cdot} = 9.2 \times 10^{-3}$. It is thus very likely that the segregation effect is operative in the present microemulsion systems, where SG1: $\bar{n}_{p\cdot} \approx 1.8 \times 10^{-5}$ (SG1) and 3.6×10^{-6} (TIPNO). Now, if the segregation effect is operative, $R_{p,microemulsion}$ would be expected to be greater than $R_{p,bulk}$ unless the confined space effect on deactivation is stronger than the segregation effect on termination. In the absence of a deactivation step (i.e., as in conventional nonliving radical polymerization), a microemulsion polymerization is very rapid due to the segregation effect causing a reduction in the termination rate. The fact that $R_{p,microemulsion} < R_{p,bulk}$ (Figure 1) thus suggests that the confined space effect on deactivation dominates. According to the simulations, the confined space effect leads to an increase in the deactivation rate for $d <$ approximately 65 nm (Figure 13). At $d = 40$ nm, the simulations indicate that deactivation is increased by a factor of 8.7 relative to bulk ($R_{deact}^c/R_{deact}^{nc} = 8.7$).

Conclusions

Microemulsion polymerizations of S at 100 °C using the cationic emulsifier TTAB have been carried out using two nitroxides of different water solubilities (SG1: relatively high water solubility; TIPNO: relatively low water solubility). All polymerizations proceeded with good control/livingness, but the AIBN initiator efficiency was markedly lower in microemulsion (0.53) than bulk (0.98). For both nitroxides, R_p was lower in microemulsion than in bulk, and the MWDs were significantly narrower in microemulsion than bulk at low conversion. Two main explanations are proposed: (*i*) The lower value of f of AIBN in microemulsion than bulk leads to a higher free nitroxide concentration, which causes lower R_p and narrower MWD. (*ii*) Compartmentalization is the second. The confined space effect acts on deactivation, exerting a stronger influence on R_p than the segregation effect on termination, resulting in a reduction in R_p and narrower MWD. The reduction in f would most likely be mainly a result of the confined space effect increasing the rate of geminate termination of AIBN radicals, i.e. point *i* is also a manifestation of compartmentalization.

Specifically designed microemulsion NMP experiments revealed that the nitroxide TEMPO can diffuse between monomer-swollen micelles on the time scale of approximately 15 min or less. The extent of retardation relative to bulk was much more severe for the less water-soluble nitroxide TIPNO than for SG1, consistent with TIPNO undergoing less exit from the particles to the aqueous phase.

Modeling and simulations (not accounting for phase transfer events) indicated that particle diameters less than approximately 15−20 nm would be required for the confined space effect to exert an influence on the deactivation reaction, to be compared with the experimental particle diameters of 20−25 nm for both nitroxides at low (< 20%) conversion.

The present work illustrates that NMP in dispersed systems (nanoreactors) can proceed significantly differently from the homogeneous counterpart. By careful choice of polymerization conditions and particle size, it is possible to exploit particle size effects to improve the level of control and livingness.

Acknowledgment. This work was partially supported by a Grant-in-Aid for Scientific Research (19550125) from the Japan Society for the Promotion of Science (JSPS), and a Kobe University Takuetsu-shita Research Project grant. We are thankful to

Prof. Yozo Miura (Osaka City University, Japan) for providing the nitroxide TIPNO. Prof. Bernadette Charleux (University of Paris, France) is acknowledged for useful discussions that led to the microemulsion polymerizations investigating partitioning effects.

References and Notes

(1) Braunecker, W. A.; Matyjaszewski, K. *Prog. Polym. Sci.* **2007**, *32*, 93–146.
(2) Zetterlund, P. B.; Kagawa, Y.; Okubo, M. *Chem. Rev.* **2008**, *108*, 3747–3794.
(3) Cunningham, M. F. *Prog. Polym. Sci.* **2008**, *33*, 365–398.
(4) Butte, A.; Storti, G.; Morbidelli, M. *DECHEMA Monogr.* **1998**, *134*, 497–507.
(5) Charleux, B. *Macromolecules* **2000**, *33*, 5358–5365.
(6) Zetterlund, P. B.; Okubo, M. *Macromolecules* **2006**, *39*, 8959–8967.
(7) Kagawa, Y.; Zetterlund, P. B.; Minami, H.; Okubo, M. *Macromol. Theory Simul.* **2006**, *15*, 608–613.
(8) Zetterlund, P. B.; Okubo, M. *Macromol. Theory Simul.* **2007**, *16*, 221–226.
(9) Maehata, H.; Buragina, C.; Cunningham, M.; Keoshkerian, B. *Macromolecules* **2007**, *40*, 7126–7131.
(10) Tobita, H.; Yanase, F. *Macromol. Theory Simul.* **2007**, *16*, 476–488.
(11) Tobita, H. *Macromol. Theory Simul.* **2007**, *16*, 810–823.
(12) Simms, R. W.; Cunningham, M. F. *Macromolecules* **2008**, *41*, 5148–5155.
(13) Delaittre, G.; Charleux, B. *Macromolecules* **2008**, *41*, 2361–2367.
(14) Zetterlund, P. B.; Okubo, M. *Macromol. Theory Simul.* **2009**, *18*, 277–286.
(15) Zetterlund, P. B.; Kagawa, Y.; Okubo, M. *Macromolecules* **2009**, *42*, 2488–2496.
(16) Fischer, H. *Chem. Rev.* **2001**, *101*, 3581–3610.
(17) Georges, M. K.; Veregin, R. P. N.; Kazmaier, P. M.; Hamer, G. K. *Macromolecules* **1993**, *26*, 2987–2988.
(18) Hawker, C. J.; Bosman, A. W.; Harth, E. *Chem. Rev.* **2001**, *101*, 3661–3688.
(19) Matyjaszewski, K.; Xia, J. H. *Chem. Rev.* **2001**, *101*, 2921–2990.
(20) Kamigaito, M.; Ando, T.; Sawamoto, M. *Chem. Rev.* **2001**, *101*, 3689–3745.
(21) Nicolas, J.; Charleux, B.; Guerret, O.; Magnet, S. *Macromolecules* **2005**, *38*, 9963–9973.
(22) Lansalot, M.; Farcet, C.; Charleux, B.; Vairon, J. P.; Pirri, R.; Tordo, P., Nitroxide-mediated controlled free-radical emulsion and miniemulsion polymerizations of styrene. In *Controlled/living radical polymerization: Progress in ATRP, NMP and RAFT*; Matyjaszewski, K., Ed.; ACS Symposium Series 768; American Chemical Society: Washington, DC, 2000; pp 138−151.
(23) Goto, A.; Fukuda, T. *Prog. Polym. Sci.* **2004**, *29*, 329–385.
(24) Candau, F., Microemulsion polymerization. In *Polymeric dispersions: Principles and applications*, Asua, J. M., Ed.; Kluwer Academic Publishers: Dordrecht, The Netherlands, 1997; pp 127−140.
(25) Chow, P. Y.; Gan, L. M. *Adv. Polym. Sci.* **2005**, *175*, 257–298.
(26) Wakamatsu, J.; Kawasaki, M.; Zetterlund, P. B.; Okubo, M. *Macromol. Rapid Commun.* **2007**, *28*, 2346–2353.
(27) Goto, A.; Kwak, Y.; Yoshikawa, C.; Tsujii, Y.; Sugiura, Y.; Fukuda, T. *Macromolecules* **2002**, *35*, 3520–3525.
(28) Cuervo-Rodriguez, R.; Bordegé, V.; Fernández-Monreal, M. C.; Fernández-García, M.; Madruga, E. L. *J. Polym. Sci.; Part A: Polym. Chem.* **2004**, *42*, 4168–4176.
(29) Benoit, D.; Chaplinski, V.; Braslau, R.; Hawker, C. J. *J. Am. Chem. Soc.* **1999**, *121*, 3904–3920.
(30) Luo, Y.; Schork, F. J. *J. Polym. Sci.; Part A: Polym. Chem.* **2002**, *40*, 3200–3211.
(31) Pan, G.; Sudol, E. D.; Dimonie, V. L.; El-Aasser, M. S. *J. Polym. Sci.; Part A: Polym. Chem.* **2004**, *42*, 4921–4932.
(32) Nomura, M.; Suzuki, K. *Ind. Eng. Chem. Res.* **2005**, *44*, 2561–2567.
(33) Alam, M. N.; Zetterlund, P. B.; Okubo, M. *Polymer* **2008**, *49*, 883–892.
(34) Wulkow, M. *Macromol. React. Eng.* **2008**, *2*, 461–494.
(35) Hui, A. W.; Hamielec, A. E. *J. Appl. Polym. Sci.* **1972**, *16*, 749–769.
(36) Khuong, K. S.; Jones, W. H.; Pryor, W. A. *J. Am. Chem. Soc.* **2005**, *127*, 1265–1277.
(37) Marque, S.; LeMercier, C.; Tordo, P.; Fischer, H. *Macromolecules* **2000**, *33*, 4403–4410.
(38) Nilsen, A.; Braslau, R. *J. Polym. Sci.; Part A: Polym. Chem.* **2006**, *44*, 697–717.
(39) Dixon, K. W., Decomposition rates of Organic Free Radical Initiators. In *Polymer Handbook*, 4th ed.; Brandrup, J., Immergut, E. H., Grulke, E. A., Eds.; Wiley: New York, 1999; p II/12.
(40) Buback, M.; Gilbert, R. G.; Hutchinson, R. A.; Klumperman, B.; Kuchta, F. D.; Manders, B. G.; O′Driscoll, K. F.; Russell, G. T.; Schweer, J. *Macromol. Chem. Phys.* **1995**, *196*, 3267–3280.
(41) Buback, M.; Kowollik, C.; Kurz, C.; Wahl, A. *Macromol. Chem. Phys.* **2000**, *201*, 464–469.
(42) Heberger, K.; Fischer, H. *Int. J. Chem. Kinet.* **1993**, *25*, 249–263.
(43) Goto, A.; Fukuda, T. *Macromol. Chem. Phys.* **2000**, *201*, 2138–2142.
(44) Yoshikawa, C.; Goto, A.; Fukuda, T. *Macromolecules* **2002**, *35*, 5801–5807.
(45) Buback, M.; Egorov, M.; Gilbert, R. G.; Kaminsky, V.; Olaj, O. F.; Russell, G. T.; Vana, P.; Zifferer, G. *Macromol. Chem. Phys.* **2002**, *203*, 2570–2582.
(46) Zetterlund, P. B.; Yamauchi, S.; Yamada, B. *Macromol. Chem. Phys.* **2004**, *205*, 778–785.
(47) Zetterlund, P. B.; Yamazoe, H.; Yamada, B.; Hill, D. J. T.; Pomery, P. J. *Macromolecules* **2001**, *34*, 7686–7691.
(48) Sobek, J.; Martschke, R.; Fischer, H. *J. Am. Chem. Soc.* **2001**, *123*, 2849–2857.
(49) Ma, J. W.; Cunningham, M. F.; McAuley, K. B.; Keoshkerian, B.; Georges, M. K. *Macromol. Theory Simul.* **2002**, *11*, 953–960.
(50) Zetterlund, P. B.; Okubo, M. *Macromol. Theory Simul.* **2005**, *14*, 415–420.
(51) Nakamura, T.; Zetterlund, P. B.; Okubo, M. *Macromol. Rapid Commun.* **2006**, *27*, 2014–2018.
(52) Zetterlund, P. B.; Nakamura, T.; Okubo, M. *Macromolecules* **2007**, *40*, 8663–8672.
(53) Lin, M.; Hsu, J. C. C.; Cunningham, M. F. *J. Polym Sci.; Part A: Polym. Chem.* **2006**, *44*, 5974–5986.